Cellular and Molecular Life Sciences (2025) 82:145
https://doi.org/10.1007/s00018-025-05649-1

Cellular and Molecular Life Sciences

ORIGINAL ARTICLE

Syndecan-3 positively regulates the pro-inflammatory function of macrophages

So Young Lee[1] · **Endika Prieto-Fernández**[2] · **Leire Egia-Mendikute**[1] · **Asier Antoñana-Vildosola**[1] · **Paloma Velasco-Beltrán**[1] · **Alexandre Bosch**[1] · **Borja Jimenez-Lasheras**[1] · **Ander de Blas**[1] · **Jone Etxaniz-Diaz de Durana**[1] · **Eunate Valdaliso-Díez**[1] · **Laura Bozal-Basterra**[3] · **Amaia Ercilla**[3] · **José Ezequiel Martin**[6] · **Arkaitz Carracedo**[3,4] · **Alena Gros**[2] · **Ana M. Aransay**[5,6] · **Asís Palazón**[1,4] · **Lorena Pérez-Gutiérrez**[1]

Received: 8 August 2024 / Revised: 10 January 2025 / Accepted: 6 March 2025

Abstract

The tumour microenvironment (TME) is a highly structured ecosystem that surrounds a tumour and plays a crucial role in tumorigenesis. As one of the most abundant cell types in the TME, tumour-associated-macrophages (TAMs) can promote disease progression and resistance to therapy. Syndecan-3 (SDC3) is a cell-surface heparan sulphate proteoglycan expressed by TAMs, although its functional relevance in these cells remains unknown. Here, we demonstrated that pro-inflammatory cytokines drive the expression of SDC3 on the cell surface of macrophages. Genetic ablation of *SDC3* in macrophages led to aberrant proliferation, adhesion and expression of CD40 and CD86 surface markers. Moreover, *SDC3* defective macrophages exhibited distinctive gene expression patterns, leading to impaired tumour cell phagocytosis and increased tumour cell proliferation. Mechanistically, a decrease in the secretion of pro-inflammatory cytokines was observed in *SDC3* KO macrophages, concomitant with impaired T cell effector functions. Additionally, a higher angiogenic capacity was observed in endothelial cells when co-cultured with macrophages deficient for *SDC3*, possibly mediated through an increased release of VEGFA, PECAM-1 and IL-8 by *SDC3* KO cells. Collectively, we have identified SDC3 as a modulator of macrophage functions aiming at supporting a pro-inflammatory and anti-tumour phenotype in these cells.

Keywords Innate immunity · Cancer · Syndecans · Immunotherapy · Angiogenesis.

Introduction

The tumour microenvironment (TME), composed of cancer cells, immune cells, stromal cells and the extracellular matrix (ECM), plays an integral role in tumorigenesis and malignant progression [1]. Tumour-associated macrophages (TAMs) are the most abundant population of tumour-infiltrating immune cells in the TME and are crucial for regulating T cell function, angiogenesis, ECM remodelling and metastasis [2]. Historically, TAMs have been categorized

---

✉ Asís Palazón
apalazon@cicbiogune.es

✉ Lorena Pérez-Gutiérrez
lperez@cicbiogune.es

[1] Cancer Glycoimmunology Lab, Center for Cooperative Research in Biosciences (CIC bioGUNE), Basque Research and Technology Alliance (BRTA), Derio, Bizkaia 48160, Spain

[2] Tumor Immunology and Immunotherapy Lab, Vall d'Hebron Institute of Oncology (VHIO), Vall d'Hebron Barcelona Hospital Campus, Barcelona, Spain

[3] Cancer Cell Signaling and Metabolism Lab, Center for Cooperative Research in Biosciences (CIC bioGUNE), Basque Research and Technology Alliance (BRTA), Derio, Bizkaia 48160, Spain

[4] Ikerbasque, Basque Foundation for Science, Bilbao, Spain

[5] Centro de Investigación Biomédica en Red de Enfermedades Hepáticas y Digestivas (CIBEREHD), Instituto de Salud Carlos III, Madrid, Spain

[6] Genome Analysis Platform, CIC bioGUNE, Bizkaia Technology Park, Derio, Bizkaia, Spain

into M1 or classically-activated macrophages, and M2 or alternatively-activated macrophages [3, 4]. In general, M1 polarization has been defined by the expression of CD40, CD86, MHC-II and iNOS, and correlates with pro-inflammatory or anti-tumour functions, including cancer cell phagocytosis and T cell recruitment. Conversely, M2 macrophages tend to exert a tumour-promoting phenotype and are characterized by the expression of CD206, CD163 and VEGFA. Nevertheless, this dichotomy is rarely reflected in the *in vivo* phenotypes of TAMs [5]. Indeed, recent studies have demonstrated that not all tumour-promoting TAMs present *bona fide* M2-like phenotypes, determining that TAMs exhibit a high degree of plasticity and are capable of displaying different phenotypes depending on their surroundings [6, 7]. Given such unique roles in tumour progression and growth, TAMs have been targeted with novel immunotherapeutic agents, including inhibitors of macrophage polarisation, macrophage depletion and monoclonal antibodies targeting cell-surface receptors. Overall, although these strategies still have to demonstrate major therapeutic impacts, the modulation of macrophages holds promise for cancer treatment [8, 9].

Syndecans (SDCs) are a family of type I transmembrane heparan sulphate proteoglycans (HSPGs) consisting of four members: SDC1-4. The core protein of these proteoglycans comprises a highly conserved cytoplasmic domain, a single transmembrane domain and a larger N-terminal extracellular domain where several glycosaminoglycan (GAG) chains are attached [10]. Through the GAG chains, SDCs interact with a range of extracellular matrix molecules, growth factors, adhesion receptors, cytokines, chemokines and other proteinases, mediating both cell–cell and cell–matrix interactions. As a result, SDCs participate in a wide range of signalling events leading to cell adhesion, angiogenesis, tumour development, inflammation and tissue repair [11–15]. Based on protein sequence homology, the four family members are divided into two sub-families, whereby SDC1 and SDC3 form the first subfamily and SDC2 and SDC4 form the other. However, their expression in different tissues is distinct from this classification. SDC1 is constitutively expressed in epithelial and plasma cells, whereas SDC2 is mainly expressed in mesenchymal cells, such as fibroblasts and smooth muscle cells. SDC3 has been mainly found in neural tissues and developing musculoskeletal tissues, and the expression of SDC4 is ubiquitous [16]. Enhanced understanding of the regulation of SDCs has led to the discovery of novel proteoglycan functions in the modulation of cancer progression, invasion and metastasis [17]. In line with the latter, we recently demonstrated that SDC3 is expressed by TAMs and endothelial cells in the TME. Moreover, its bulk expression correlates with a better overall survival on hypoxic melanoma tumours [18]. However, the role of SDC3 on TAMs and its possible impact on tumour development and progression remain elusive. In this context, further knowledge of SDC3 could facilitate the identification of novel therapeutic targets in TAMs for cancer treatment.

Here, we investigated the role of SDC3 in the regulation of the functions of macrophages. We found that the expression of SDC3, but not the other members of the SDC family, is increased in response to pro-inflammatory/anti-tumour cytokines. Deletion of this gene resulted in reduced adhesion and expression of cell surface markers in macrophages. RNA sequencing analysis detected significant changes in pathways related to inflammation, angiogenesis and T cell activation in *SDC3* deficient macrophages. This phenotype was functionally translated into an increased tumour spheroid formation capacity and a decreased ability to phagocytose tumour cells. Mechanistically, SDC3 positively regulated the secretion of pro-inflammatory cytokines, resulting in an enhanced capacity to eliminate pathogenic bacteria. Moreover, *SDC3* deficient TAMs showed a decreased ability to activate T cells and an increased angiogenic capacity. Together, these findings reveal the ability of SDC3 to enhance the function of pro-inflammatory TAMs. Since pro-inflammatory TAMs are found to be beneficial as anti-tumour therapies [8], our results identify SDC3 as a potential target for TAM-targeted cancer immunotherapies.

Materials and methods

Cell culture

THP-1 human monocytic cell line was obtained from the American Type Culture Collection (ATCC Cat. #: TIB-202) and was cultured in RPMI 1640 GlutaMAX (Gibco Cat. #: 61870010) supplemented with 10% FBS (ThermoFisher Scientific Cat. #: 10270106) and 1% Penicillin-Streptomycin (ThermoFisher Scientific Cat. #: 15140122). MDA-MB-231 human breast cancer cell line (ATCC Cat. #: CCL-185) was cultured in DMEM F-12 K (Gibco Cat. #: 31331028) supplemented with 10% FBS (ThermoFisher Scientific Cat. #: 10270106) and 1% Penicillin-Streptomycin (ThermoFisher Scientific Cat. #: 15140122). MDA-MB-231 cells were transduced with a lentivirus expressing luciferase-GFP and sorted to generate MDA-MB-231-GFP cells, that were cultured as above. Human Umbilical Vein Endothelial Cells (HUVEC Promocell Cat. #: C-12203) were cultured in Endothelial Cell Growth Medium (ECM, Promocell Cat. #: C-22010) containing 10% FBS and grown in 1% pig gelatin (Sigma Cat. #: G9391)-coated plates. All cells were maintained at 37 °C in a 5% CO_2 atmosphere.

Macrophage differentiation and polarization

1.5×10^6 cells THP-1 cells were differentiated with 20 ng/ml of phorbol 12-myristate 13-acetate (PMA, Sigma Cat. #: 524400) for 24 h in 6-well plates. After 24 h, the medium was changed. The following day, differentiated THP-1 macrophages were polarized adding recombinant human IFNγ (100 ng/mL, Biolegend Cat. #: 570206), IL-4 (20 ng/ml, Miltenyi Biotec S.L Cat. #: 130-112-411), or IL-13 (20 ng/ml, Miltenyi Biotec S.L Cat. #: 130-094-117) for a further 24, 48–72 h.

Knockout of *SDC3* by CRISPR/Cas9

Deletion of *SDC3* in THP-1 cells was performed using the following TrueGuide Synthetic gRNAs (sgRNAs) from ThermoFisher Scientific: CRISPR923443_SGM TrueGuide Synthetic sgRNA SDC3 (target DNA sequence: AACTGG ATGACCTCTACTCG Cat. #: A35511) targeting the exon 2 of human *SDC3* gene. Ribonucleoprotein (RNP) complexes were generated with 30 pmol of TrueCut Cas9 protein v2 (Invitrogen Cat. #: A36496) and 30 pmol of sgRNA. RNP complexes were introduced into cells using the Neon transfection system (Invitrogen Cat. #: MPK 1025) following the manufacturer's instructions. 72 h after transfection, single-cell dilutions were performed in 96-well plates by sorting of transduced cells with a BD FACSAria Fusion sorter (BD Biosciences) (purity > 95%). Cells were grown and the absence of *SDC3* was confirmed in each clone by Western blot.

Overexpression of *SDC3*

For *SDC3* overexpression, the codon-optimized sequence of human full-length SDC3-3xFlag was synthetized and subcloned into a puromycin lentiviral vector: pLV-MSCV (Genscript). For the generation of lentiviral particles, 50–70% confluent HEK293T cells were transfected with JetPEI kit (Polyplus transfection #101–10 N) using a mix of lentiviral plasmids: 4 ug of psPAX2 (Addgene plasmid Cat. #: 12260), 1.5 ug of VSV-G (Addgene plasmid Cat. #: 8454) and 5 ug of *SDC3* of the plasmid. After 48 h, lentiviral particles were harvested from the supernatant, filtered through a 0.45 µm filter and transduced into *SDC3* KO THP-1 cells. *SDC3* KO OE THP-1 cells were selected with 1.0 µg puromycin.

Isolation and culture of CD8$^+$ T cells

With the approval of the Ethical and Scientific Committees (code CEIC E19-75), human peripheral blood mononuclear cells (PBMCs) were isolated from buffy coats provided by the Basque Biobank by Ficoll-Paque Plus (Cytiva Cat. #: 17144003) density centrifugation (1200 g for 10 min at RT) using SepMat-50 tubes (StemCell Cat. #: 85450). CD8$^+$ T cells were magnetically isolated using the EasySep Human CD8$^+$ T Cell Isolation Kit (StemCell Cat. #: 17953RF) and a RoboSep cell separator (StemCell) according to the manufacturer's indications. Human CD8$^+$ T cells were grown in OpTmizer™ CTS medium (ThermoFisher Scientific Cat. #: A1048501) supplemented with CTS Immune Cell Serum Replacement (ThermoFisher Scientific Cat. #: A2596101) and hIL2 (100 IU/ml, Miltenyi Biotec Cat. #: 097–743). For macrophage-T cell co-cultures, on the day of the experiment, 300.000 CD8$^+$ T cells were added to 500.000 previously differentiated THP-1 macrophages in media containing 5 µg/ml of anti-CD3 (BD Biosciences Cat. #: 567118). CD8$^+$ T cells were collected after 4 days and analysed by flow cytometry. For some of the conditions, CD8$^+$ T cells were first pelleted and mixed with 5 µM of CFSE reagent (ThermoFisher Scientific Cat. #: C34554) for 7 min at 37 °C in the dark, followed by two washes, before incubation for 4 days.

Flow cytometry

Cells were blocked with a TruStain FcX blocker (Biolegend Cat. #: 101320) for 10 min at RT, followed by an incubation in the presence of fluorochrome-conjugated antibodies (listed in Supplementary Table 1) in flow cytometry staining buffer (Invitrogen Cat. #: 00-4222-26) for 30 min at 4°C in the dark. DAPI (ThermoFisher Scientific Cat. #: D1306) was used as a viability dye. Cells were acquired in a BD FACS Symphony A3 flow cytometer.

Cytokine quantification and ELISAs

Quantification of cytokines was performed with the LEGENDplex™ HU Essential Immune Response Panel. Briefly, beads pre-coated with antibodies for IL-4, IL-2, CXCL10 (IP-10), IL-1β, TNF-α, CCL2 (MCP-1), IL-17 A, IL-6, IL-10, IFNγ, IL-12p70, CXCL8 (IL-8) and Free Active TGF-β1, were incubated with cell supernatants. Once the analyte was bound, a cocktail of biotinylated antibodies was added, followed by PE-Streptavidin, which served to quantify cytokine concentrations alongside a standard curve by flow cytometry. Quantification of angiogenic factors was performed with the LEGENDplex™ Human Angiogenesis Panel 1. Briefly, beads pre-coated with antibodies for IL-6, Angiopoietin-1, Angiopoietin-2, EGF, FGF-basic, CXCL8 (IL-8), PECAM-1, PlGF, VEGF, TNF-α were incubated with cell supernatants. Once the analyte was bound, a cocktail of biotinylated antibodies was added, followed by PE-Streptavidin, which served to quantify cytokine concentrations alongside a standard curve by flow cytometry.

Levels of VEGFA on cell supernatants were analysed using the Human VEGF ELISA Kit (R&D Systems Cat. #: DVE00), as per manufacturer´s instructions. Levels of TNF on cell supernatants were analysed using the Human TNF-alpha DuoSet ELISA (R&D Systems Cat. #: DY210), as per manufacturer´s instructions.

Western blot

Total cells were collected using 2 mM EDTA for 10 min, centrifuged and lysed with RIPA buffer (ThermoFisher Scientific Cat. #: 89900). Protein quantification was performed using the Pierce BCA Protein Assay Kit (ThermoFisher Scientific Cat. #: 23227). The procedure was followed as previously described [19]. Band intensities were determined by densitometric analysis using FIJI software.

Immunofluorescence (IF)

THP-1 cells were polarized on coverslips as described above and fixed in ice-cold methanol for 10 min. Next, permeabilization was performed using 0.1% triton X-100 for 5 min at RT, followed by blocking with 3% BSA for 15 min at RT. SDC3 primary antibody (R&D Systems Cat. #: AF3539), was incubated overnight at 4 °C in blocking buffer. The next day, coverslips were incubated with secondary anti-goat 555 antibody and DAPI for 2 h at RT, followed by washing and mounting with a ProLong gold antifade reagent. In some experiments, Phalloidin (Sigma Cat. #: P1951) was included with the secondary antibodies.

RT-qPCR

Total mRNA was extracted using the NucleoSpin RNA kit (Macherey-Nagel Cat. #: 740955.250), following manufacturer´s instructions. cDNA was synthesized using 1 µg of purified mRNA with M-MLV reverse transcriptase (ThermoFisher Scientific Cat. #: 28025-013) and random primers (ThermoFisher Scientific Cat. #: 58875) following manufacturer's instructions. RT-qPCR was performed in a Real-Time PCR System (ThermoFisher Scientific) using PerfeCTa SYBR Green SuperMix reagent (Quantabio Cat. #: 95056-500) and gene-specific primers (Supplementary Table 2). Data was analyzed using QuantStudio version 1.3 (ThermoFisher Scientific), as described in previous work [19].

RNA sequencing and analysis (RNAseq)

Total mRNA was extracted using the NucleoSpin RNA kit (Macherey-Nagel Cat. #: 740955.250). RNA sample quantity and quality were evaluated using Qubit RNA HS Assay Kit (ThermoFisher Scientific Cat. #: Q32855) and Agilent RNA 6000 Nano Chips (Agilent Technologies Cat. #: 5067−1511), respectively. A total of 1 ug of mRNA was isolated, fragmented and primed. The first cDNA strand was synthesized with SuperScript-II Reverse Transcriptase (ThermoFisher Scientific Cat. #: 18064-014) and libraries were prepared using TruSeq Stranded mRNA library Prep kit (Illumina Inc. Cat. #: 20020594) and TruSeq RNA CD Index Plate (96 Indexes, 96 samples, Illumina Inc. Cat. #: 20019792), following the TruSeq Stranded mRNA Sample Preparation Guide (Part #15031058 Rev. E). The final dsDNA libraries were quantified by Qubit dsDNA HS DNA Kit (ThermoFisher Scientific Cat. #: Q32854) and qualified by an Agilent 2100 Bioanalyzer using Agilent High Sensitivity DNA kit (Agilent Technologies Cat. #: 5067−4626). Illumina 100 nucleotides paired-end sequencing was performed in a NovaSeq6000 (Illumina Inc.).

For the RNAseq analysis, sequencing data were converted into raw data (FASTQ files) using the Illumina bcl2fastq Conversion Software. QC and metric calculation of all fastq files were done with fastQC version v0.11.6. Compilation for inspection of all fastQC reports was done using multiQC version 1.13. Adapter trimming was performed using fastp version 0.23.2. Alignments of the reads into the reference genome hg38.bwa was performed using STAR version 2.7.10b. PCR Duplicates were removed from aligned BAM files with picard version 2.27.5 using the MarkDuplicates command. Additional statistics and information on the processed BAM files for inspection were obtained using samtools version 1.16.1 using the flagstat command and picard version 2.27.5. Indexing aligned BAM files was done using samtools version 1.16.1. Reads for analysed features were assigned and counted from the processed BAM files using SubRead's FeatureCounts version v2.0.3. Differential gene expression analysis was performed by the DESeq2 version 1.40.2 [REF]. GSEA was performed in R using *fgsea* [20] and MSigDBR [21] packages. Hallmark and C2 to C7 gene collections were used. Volcano plots were generated using the ggplot2 package. The data is available and has been uploaded into the GEO repository (GEO accession GSE273450).

Phagocytosis assays

For the *S. aureus* particle phagocytosis assay, ThermoFisher Scientific Nunclon Sphere (ThermoFisher Scientific Cat. #: 174929) U-shape 96-well plate was used. 100 µl containing 200.000 WT or *SDC3* KO THP-1 cells were incubated in each well with 100 µl of pHrodo™ Green *S. aureus* bioparticles (ThermoFisher Scientific Cat. #: P35367) for 1 h at 37 °C. pHrodo bioparticles are non-fluorescent outside the cell at neutral pH but fluoresce brightly in acidic pH environments, such as those of endosomes and lysosomes. To inhibit phagocytosis, cells were pre-treated with 10 µM Cytochalasin D (ThermoFisher Scientific Cat. #: PHZ1063). After 1 h, cells were collected for flow cytometry analysis and green fluorescence within THP-1 cells was calculated, normalized to the WT condition. Part of the sample was collected, stained with DAPI and Phalloidin, and cytospined onto slides. Slides were then fixed with ProLong gold antifade reagent (ThermoFisher Scientific, Cat. #: P3693), before acquisition with a Leica SP8 Lightning confocal microscope. For the cancer cell phagocytosis assay, 30.000 MDA-MB-231-GFP cells and 100.000 THP-1 WT or *SDC3* KO cells were co-cultured in a U-shaped 96-well ThermoFisher Scientific Nunclon Sphere plate (ThermoFisher Scientific Cat. #: 174929). The mixture was incubated at 37 °C overnight. The next day, the cells were collected for flow cytometry analysis and GFP within THP-1 cells was used to calculate phagocytosis rate, normalised to the MDA-MB-231-GFP cells. Part of the sample was collected, stained with DAPI and cytospined onto slides. Slides were then fixed with ProLong gold antifade reagent (ThermoFisher Scientific, Cat. #: P3693), before acquisition with a Leica SP8 Lightning confocal microscope.

Breast cancer cell spheroid formation and proliferation assays

2.000 MDA-MB-231-GFP and THP-1 WT or *SDC3* KO cells were co-cultured in a 96-well U-shaped plate (ThermoFisher Scientific Cat. #: 174929) and incubated at 37 °C to let spheroids naturally form. Pictures were taken every day in a Nikon Eclipse TS100 microscope. After 7 days of incubation, spheroids were collected for proliferation analysis by flow cytometry using counting beads (Invitrogen Cat. #: C36950).

Cell adhesion assay

THP-1 cells (150.000 cells/well) were cultured using a 48-well plate (Corning Cat #: 3548) in medium without FBS containing 2mM $CaCl_2$, 2mM $MgCl_2$ and 20 ng/ml of PMA for 1 h at 37 °C, followed by washing and staining with 0.2% crystal violet (Sigma Cat #: C6158). Stained cells were further lysed with 10% acetic acid and the optical density (OD) was measured at 595 nm in a PerkinElmer Victor Nivo multi-plate reader.

Cell proliferation

1×10^6 THP-1 WT, *SDC3* KO and *SDC3* KO OE cells were cultured in 7 ml of culture medium. Cell numbers were counted daily using an automated cell counter Countess 3 instrument (ThermoFisher Scientific product number: AMQAX2000).

Proteome profiler array

Differentiated WT and *SDC3* KO THP-1 macrophages were polarized with 100 ng/ml of IFNγ for 2 h. Cells were collected with TrypLE (Gibco Cat. #: 2785288) and washed twice with PBS. For phospho-kinase identification, the Proteome Profiler Human Phospho-Kinase Array Kit was used (R&D Systems Cat. #: ARY003C) following the manufacturer's instructions.

Tube formation assay

96-well plates (Corning Cat. #: 3595) were pre-coated with 50 µl of Matrigel (Corning Cat. #: 356231) for 1 h at 37 °C. HUVECs were dissociated with Trypsin-EDTA (0,25%) (ThermoFisher Scientific Cat. #: 25200056) and 30.000 cells were resuspended in 150 µl of THP-1 WT/KO-conditioned medium for 24 h at 37 °C. Tube formation was photographed under an Olympus IX-83 inverted microscope and analysed with FIJI software.

Cell migration assay

Cell migration was analysed using the xCELLigence Cell Invasion & Migration platform (Agilent). Briefly, THP-1 WT/KO conditioned medium was added to the lower chamber of Xcelligence 16-well CIM-Plates (Agilent Cat#: 5665825001). On the top chamber, 20.000 HUVECs were seeded, and migration was measured in real-time using the xCELLigence platform (Agilent), according to manufacturer´s instructions.

Statistics

Statistical analyses were performed using GraphPad PRISM 8 software (GraphPad). Plots show mean ± standard error of the mean (SEM). Comparisons between two groups were carried out using the paired Student's t test. One-way ANOVA or two-way ANOVA with Tukey's or Bonferroni′s post hoc test were performed for multiple group comparisons. Significant p values are indicated in Figure legends.

Results

IFNγ promotes the expression of Syndecan-3 on human macrophages

The plethora of cytokines produced in the TME play important roles in cancer pathogenesis. They can either promote tumour growth and facilitate metastasis, or alternatively, inhibit tumour development and progression [22]. IFNγ, a long-recognized player during cancer progression, can stimulate the cytotoxic activity of immune cells against tumour cells, resulting in anti-tumour immune responses. Additionally, it can stimulate the activity of pro-inflammatory macrophages within the TME, to inhibit tumour progression [23]. Instead, IL-4 and IL-13 promote polarization of macrophages towards an anti-inflammatory state, resulting in a tumour promoting activity [24]. To investigate the potential role of IFNγ in inducing the expression of SDCs in human macrophages, we differentiated THP-1 human monocytic cells to macrophages and analyzed the levels of expression of all members of the SDC family (Fig. 1a). Here, the expression of *SDC1* was significantly downregulated in response to IFNγ, while *SDC2* and *SDC4* remained unchanged following 24 h of stimulation. Interestingly, the expression of *SDC3* was robustly increased after IFNγ treatment, with ~ 5-fold higher expression compared to control macrophages. Of note, *SDC2*, *SDC3* and *SDC4* showed comparable absolute gene expressions, whereas the amount of *SDC1* message was notably decreased (Supplementary Fig. 1a). Given the cell surface expression of SDCs, we next sought to investigate the presence of SDC1-4 at the protein level on the cell surface of control and IFNγ-treated THP-1 macrophages by flow cytometry. IFNγ-treated macrophages showed a significant increase in cell surface expression of SDC3 at 24, 48 and 72 h, but not the other members of the family (Fig. 1b and Supplementary Fig. 1b). Notably, PMA activation has previously been associated to an induction of SDC shedding in other cell types [25], however, treatment with PMA did not induce a decrease in cell surface SDC protein levels in THP-1 cells (Supplementary Fig. 1c). To confirm the expression of SDC3 in response to pro-inflammatory cytokines, THP-1 macrophages were subsequently immunostained following 24 h of stimulation with IFNγ, revealing a clear membrane localization of SDC3 (Fig. 1c). Importantly, stimulation of macrophages with the anti-inflammatory/pro-tumour cytokine cocktail IL-4/IL-13 showed no immunostaining of SDC3. Similarly, expression of *SDC3*, but not the other *SDCs*, was upregulated in response to IFNγ in THP-1 macrophages. Interestingly, this effect was not found with IL-4/IL-13 treatment (Fig. 1d and Supplementary Fig. 1d). Overall, IFNγ induced an upregulation of SDC3, but not the other family members, suggesting that pro-inflammatory cytokines may induce SDC3 expression in macrophages.

Fig. 1 SDC3, but not the other syndecans, is upregulated in response to IFNγ in human macrophages. (**a**) *SDC1*, *SDC2*, *SDC3* and *SDC4* mRNA levels in control and IFNγ-treated THP-1 macrophages, as assessed by RT-qPCR (n=4–6). (**b**) Representative flow histograms (upper panel) and pooled data (lower panel) showing the protein expression of SDC1, SDC2, SDC3 and SDC4 in control and IFNγ-treated THP-1 macrophages (n=4–6). (**c**) Representative confocal images (n=3) of control, IFNγ- or IL-4/IL-13-treated THP-1 macrophages immunostained for DAPI and SDC3 (scale bar 5 μm). (**d**) *SDC3* mRNA levels in control, IFNγ- and IL-4/IL-13-treated THP-1 macrophages, as assessed by RT-qPCR (n=3). Means ± SEM. Statistically significant difference from controls or between indicated groups is shown by ns: not significant, $^{**}p<0.01$, $^{***}p<0.001$ and $^{****}p<0.0001$

Syndecan-3 regulates the proliferation and adhesion of macrophages

To further explore the role of SDC3 in TAMs, we generated *SDC3* KO THP-1 cells using CRISPR/Cas9 (Fig. 2a). Here, the expression of *SDC3* was completely abolished in *SDC3* KO macrophages, which was further confirmed by flow cytometry (Fig. 2b and Supplementary Fig. 2a). These cells showed no difference in the percentage of live cells compared to WTs, and the activation of common signalling pathways remained unchanged (Supplementary Fig. 2b and c). Nevertheless, the phosphorylation of PYK2, RSK1/2/3 and HSP27 kinases was increased in *SDC3* KO THP-1 cells compared to WT macrophages (Supplementary Fig. 2d).

To functionally assess the impact of *SDC3* deletion, we first analyzed the expression of the other members of the SDC family in *SDC3* KO macrophages. The expression of SDC1, 2 and 4 was not altered upon *SDC3* deletion in macrophages (Supplementary Fig. 2e). Next, we evaluated the phenotype of IFNγ-stimulated *SDC3* WT vs. KO THP-1 macrophages. While IFNγ stimulation promoted flat and pancake-like shaped macrophages characteristic of a pro-inflammatory phenotype [26], this identity was lost in *SDC3* KO macrophages, that displayed a more rounded phenotype (Fig. 2c). Moreover, *SDC3* KO THP-1 cells proliferated more compared to WT cells (Fig. 2d), in line with previously demonstrated SDC3-dependent effects in the proliferation of other cell types [27–29]. Next, given the well-established role of SDCs in cell adhesion [11], we evaluated the loss of proliferative function and increased adhesion ability of THP-1 cells in response to PMA. Here, *SDC3*-deficient macrophages showed significantly reduced adhesion capacity in response to PMA, when compared to WT THP-1 cells (Fig. 2e). To directly assess the contribution of SDC3 to the above functions, we overexpressed *SDC3* in *SDC3* KO THP-1 cells (Supplementary Fig. 3a). Here, the expression of *SDC3* was greatly increased compared to *SDC3* KO

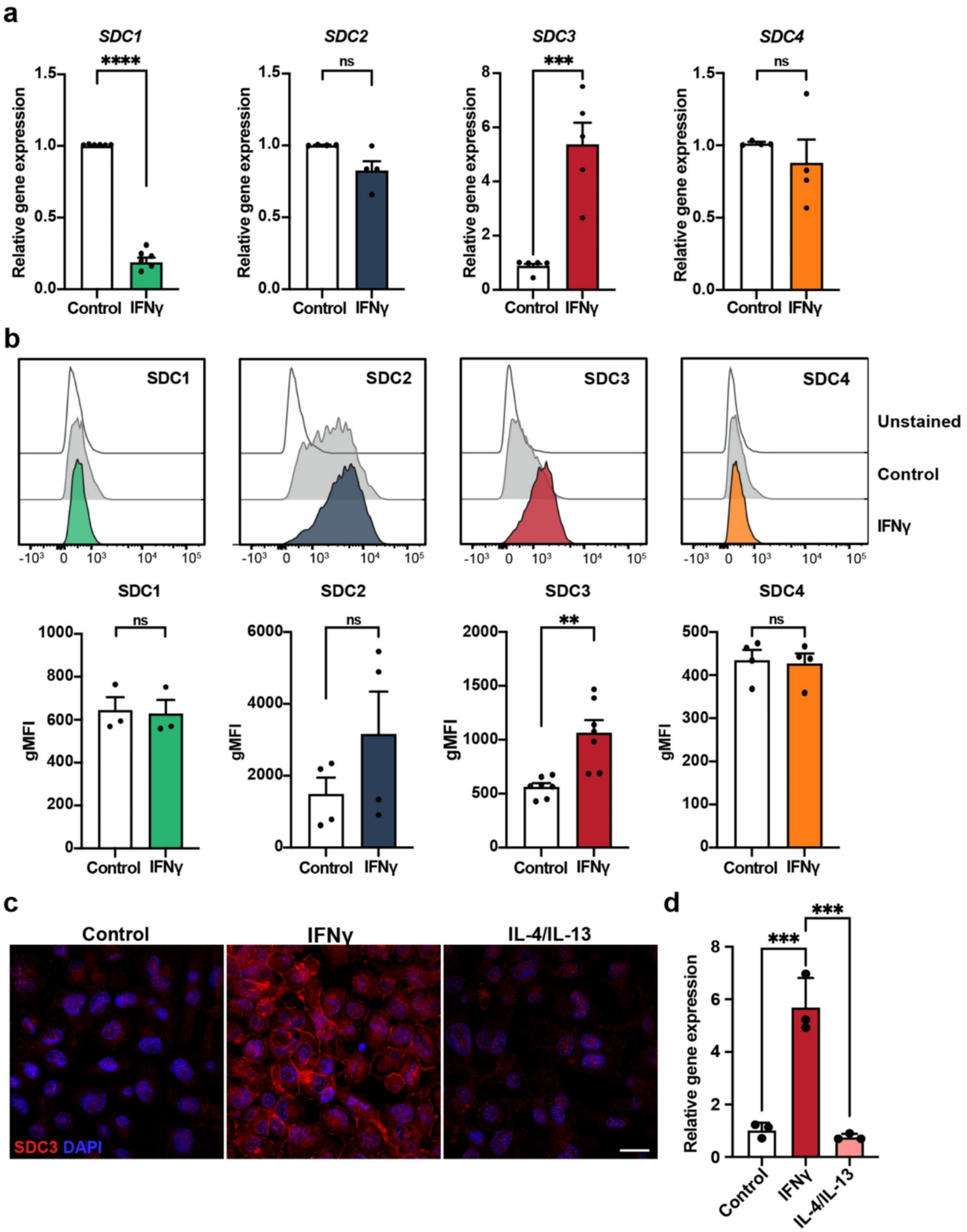

macrophages (Supplementary Fig. 3b). This strategy significantly reverted the excessive proliferation observed in *SDC3* KO cells, and partially recovered the impaired adhesion of *SDC3* KO macrophages in response to PMA (Supplementary Fig. 3c and d), suggesting a regulatory role for SDC3 in these macrophage functions. Furthermore, to gain insight

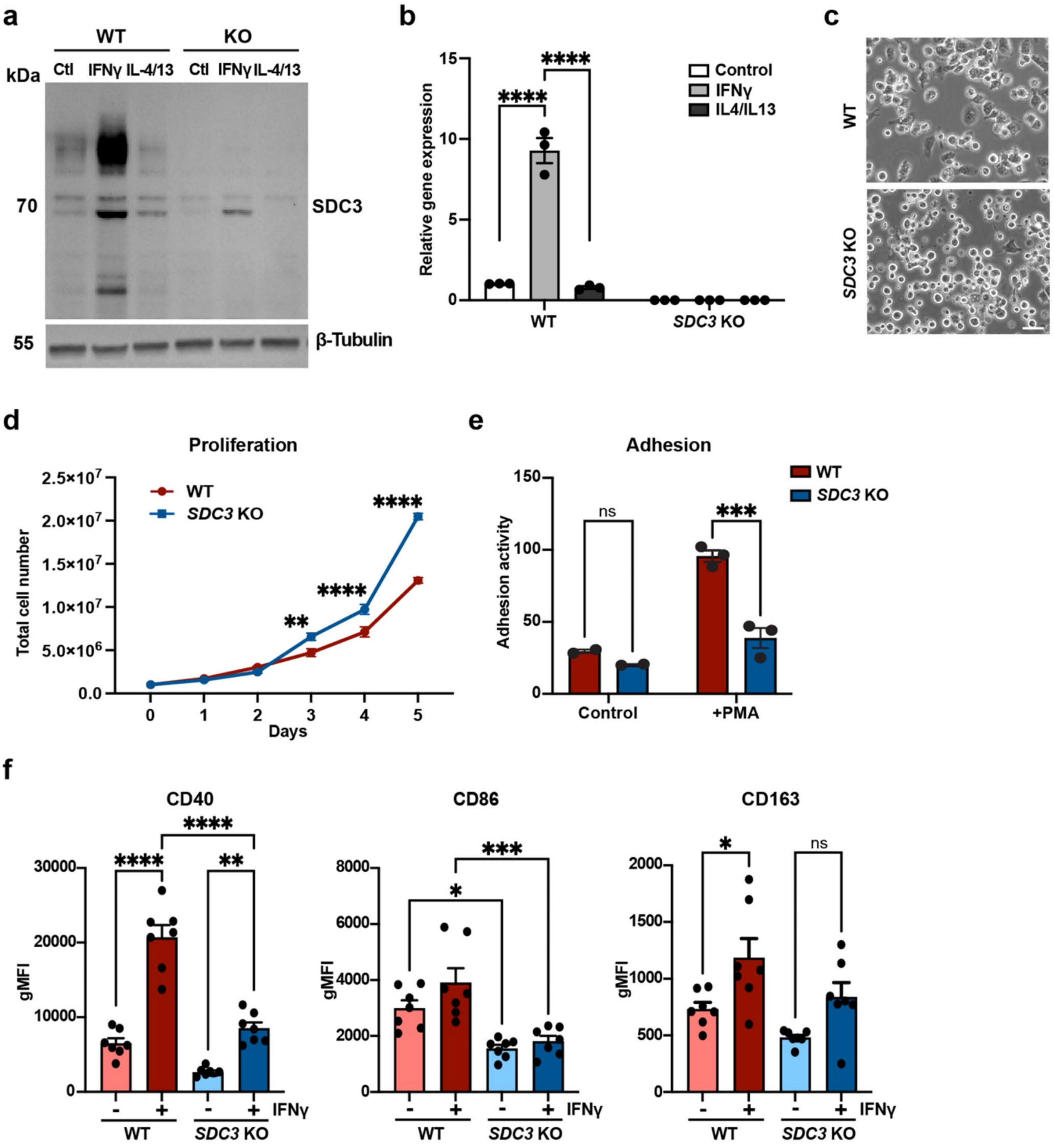

Fig. 2 SDC3 deficient macrophages exhibit aberrant proliferation, adhesion and expression of cell surface markers. (**a**) Representative immunoblots ($n=3$) of WT or *SDC3* KO THP-1 macrophages stimulated with either 100 ng/ml of IFNγ or 20 ng/ml of IL-4/IL-13 cocktail. (**b**) *SDC3* mRNA levels in control, IFNγ- and IL-4/IL-13-treated WT or *SDC3* KO THP-1 macrophages, as assessed by RT-qPCR ($n=3$) (**c**) Representative brightfield images of WT or *SDC3* KO THP-1 macrophages (scale bar 20 µm, $n=3$). (**d**) Proliferation of WT or *SDC3* KO THP-1 cells up to 5 days ($n=3$). (**e**) Adhesion activity of WT or *SDC3* KO THP-1 macrophages, as quantified by Crystal Violet ($n=2$–3). (**f**) Flow cytometry data showing the expression of CD40, CD86 and CD163 in WT or *SDC3* KO THP-1 macrophages stimulated with 100 ng/ml of IFNγ ($n=7$). Means ± SEM. Statistically significant difference from controls or between indicated groups is shown by ns: not significant, $*p<0.05$, $**p<0.01$, $***p<0.001$, and $****p<0.0001$

into potential changes in the expression of macrophage markers upon *SDC3* deletion, we applied flow cytometry to the study of classical M1- and M2-like membrane markers (Fig. 2f and Supplementary Fig. 2f). Results showed that IFNγ-stimulated *SDC3*-deficient macrophages exhibited a decrease in classical M1 markers CD40 and CD86 expression, when compared to IFNγ-stimulated WT cells. Additionally, the upregulation of CD163 observed in response to IFNγ in WT macrophages was lost in *SDC3* KO THP-1 macrophages. Altogether, *SDC3*-deficient macrophages exhibited aberrant proliferation, adhesion and expression of typical activation markers, revealing SDC3 as an effective modulator of macrophage functions.

Syndecan-3 defective macrophages show distinctive gene expression patterns

To understand the transcriptional changes governed by SDC3, we next performed RNA sequencing of WT and *SDC3* KO THP-1 macrophages in response to IFNγ. Here, several genes were found to be differentially expressed in *SDC3* KO macrophages (Fig. 3a), confirming a distinctive gene expression signature upon *SDC3* deletion. In order to understand whether these genes participated in the same biological processes, we performed gene set enrichment analysis (GSEA) (Fig. 3b and Supplementary Fig. 4) [30]. A total of 1.325 gene sets based on prior published data were analyzed, including biological pathways, response to drug

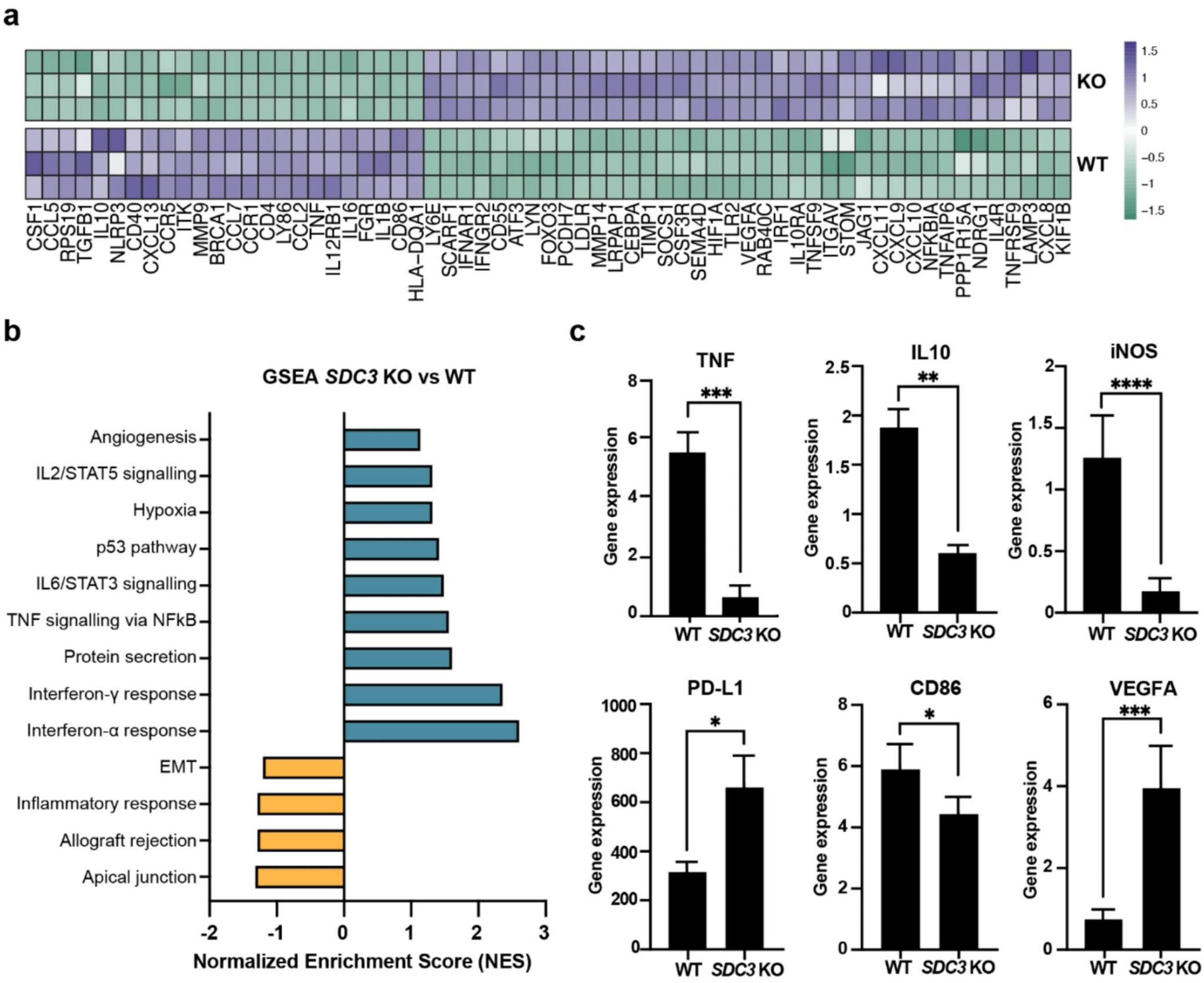

Fig. 3 *SDC3*-defective macrophages show distinctive gene expression patterns. (**a**) Heatmap of differentially expressed genes in IFNγ-treated THP-1 WT and *SDC3* KO macrophages ($n=3$, purple represents upregulation and green represents downregulation). (**b**) Differentially expressed pathways in IFNγ-treated THP-1 WT and *SDC3* KO macrophages where blue represents pathways upregulated in *SDC3* KO macrophages, and orange represents downregulated pathways in *SDC3* KO macrophages ($n=3$). (**c**) *TNF*, *IL10*, *iNOS*, *PD-L1*, *CD86*, and *VEGFA* mRNA levels in IFNγ-treated THP-1 WT and *SDC3* KO macrophages, as assessed by RT-qPCR ($n=3$). Means ± SEM. Statistically significant difference from controls or between indicated groups is shown by $^{*}p<0.05$, $^{**}p<0.01$, $^{***}p<0.001$ and $^{****}p<0.0001$

treatments, metabolic pathways, transcriptional programs and stress responses. GSEA analysis revealed that *SDC3* KO macrophages showed an upregulation of pathways related to angiogenesis, protein secretion, TNF signalling and proliferation and differentiation such as IL6/STAT3. However, pathways involved in inflammatory responses, epithelial-to-mesenchymal transition (EMT) and apical junctions were downregulated. To confirm these results, gene expression was measured in IFNγ-treated WT and *SDC3* KO THP-1 macrophages by RT-qPCR (Fig. 3c). The expression of genes related to inflammation such as *TNF*, *IL-10* or *iNOS* [31] was significantly decreased in macrophages deficient for *SDC3*. Additionally, *SDC3* KO THP-1 macrophages exhibited an upregulation of the expression of *PD-L1*, a pivotal immune checkpoint that, through binding to PD-1, controls the induction and maintenance of immune tolerance [32]. In line with this, *CD86*, an essential co-stimulatory signal for T cell activation [33], was downregulated in *SDC3*-deficient macrophages. Finally, expression of *VEGFA*, the quintessential angiogenic factor [34], was significantly higher in *SDC3* KO macrophages. Collectively, pathways related to inflammation, T cell activation and angiogenesis were altered in *SDC3*-deficient macrophages. These processes regulate TME-mediated tumour progression and growth, suggesting a role for SDC3 in tumorigenesis.

Syndecan-3 in macrophages plays a role in tumour cell phagocytosis and proliferation

Hypothesizing a link between macrophage SDC3 and tumour progression, we next assessed macrophage-mediated tumour cell phagocytosis, a key process for tumour cell-killing, antibody-dependent cellular cytotoxicity and vascular damage [35]. With this aim, IFNγ-stimulated WT or *SDC3* KO THP-1 macrophages were co-cultured with MDA-MB-231-GFP breast cancer cells, and phagocytosis was measured by flow cytometry. IFNγ-stimulated *SDC3*-deficient macrophages showed significantly decreased phagocytic capacity, with ~ 3-fold lower phagocytosis rate compared to WT cells (Fig. 4a). To investigate the role of SDC3 in tumour development in a more relevant setting, we took advantage of organoid-spheroid models that provide an *in vitro* 3D platform resembling tumour growth [36]. Briefly, MDA-MB-231-GFP cells were co-cultured with IFNγ-stimulated WT or *SDC3* KO THP-1 macrophages and after 1, 3, and 6 days, the spontaneous formation of spheroids was quantified by flow cytometry. Upon IFNγ-stimulation, *SDC3* KO macrophages promoted a significant increase in MDA-MB-231-GFP cell spheroid proliferation compared to WT cells (Fig. 4b). Overall, *SDC3* deficient macrophages exhibited reduced cancer cell phagocytic capacity and promoted tumour-cell proliferation, suggesting that SDC3 in macrophages is protective during tumour progression and growth.

Syndecan-3 enhances macrophage pro-inflammatory functions

Macrophages are vital players of the innate immune response and play pivotal roles in the regulation of inflammation [37]. As phagocytes, one of their best-established roles is to ingest and eliminate pathogens, essential for tissue homeostasis, inflammation and host defence [38]. To understand whether SDC3 may play a role in bacterial phagocytosis, the uptake of *S. aureus* bioparticles was analyzed in IFNγ-stimulated WT or *SDC3* KO THP-1 macrophages. Here, *SDC3*-deficient cells exhibited reduced phagocytosis of the Gram-positive bacteria compared to controls (Fig. 5a). Of note, while IFNγ-stimulated WT macrophages showed reduced phagocytic capacity, as previously described [39–41], the phagocytosis of *S. aureus* exerted by *SDC3*-deficient cells remained unchanged in response to IFNγ. This suggests that, upon *SDC3* deletion, the effect of IFNγ in the phagocytic capacity of macrophages is lost. The engulfment of foreign agents by macrophages is accompanied by the production and release of cytokines to mediate an effective immune response [31]. In aiming to investigate the effect of *SDC3* deletion in the release of cytokines by macrophages, we analyzed a portfolio of proteins by flow cytometry in the supernatants of IFNγ-stimulated WT or *SDC3* KO THP-1 macrophages (Fig. 5b and Supplementary Fig. 5a). MCP-1, one of the key chemokines that regulates migration and infiltration of monocytes and macrophages [42], was drastically reduced in response to IFNγ in *SDC3* deficient macrophages. Moreover, supernatants from *SDC3* KO THP-1 macrophages neglected to show IL-10 secretion, critical in limiting immune-mediated pathology [43]. In addition, the pro-inflammatory cytokine TNF was also decreased in supernatants from *SDC3*-deficient THP-1 macrophages (Supplementary Fig. 5b). Nevertheless, secretion of the neutrophil chemoattractant IL-8 was increased in IFNγ-stimulated *SDC3* KO THP-1 macrophages when compared to controls. These results are in line with the previously identified gene expression patterns observed in *SDC3* KO macrophages (Fig. 3c).

Some cytokines are sentinels of the innate immune system and mediate the transition from innate to adaptive immunity, acting as chemoattractants for T and B cells. Additionally, macrophages express major histocompatibility complex molecules on their membranes, and as such, also present antigens to lymphocytes [31]. To clarify the role of macrophage SDC3 in the regulation of T cells, we established co-cultures of IFNγ-stimulated WT or *SDC3* KO macrophages and $CD8^+$ T cells. Here, *SDC3*-deficient macrophages

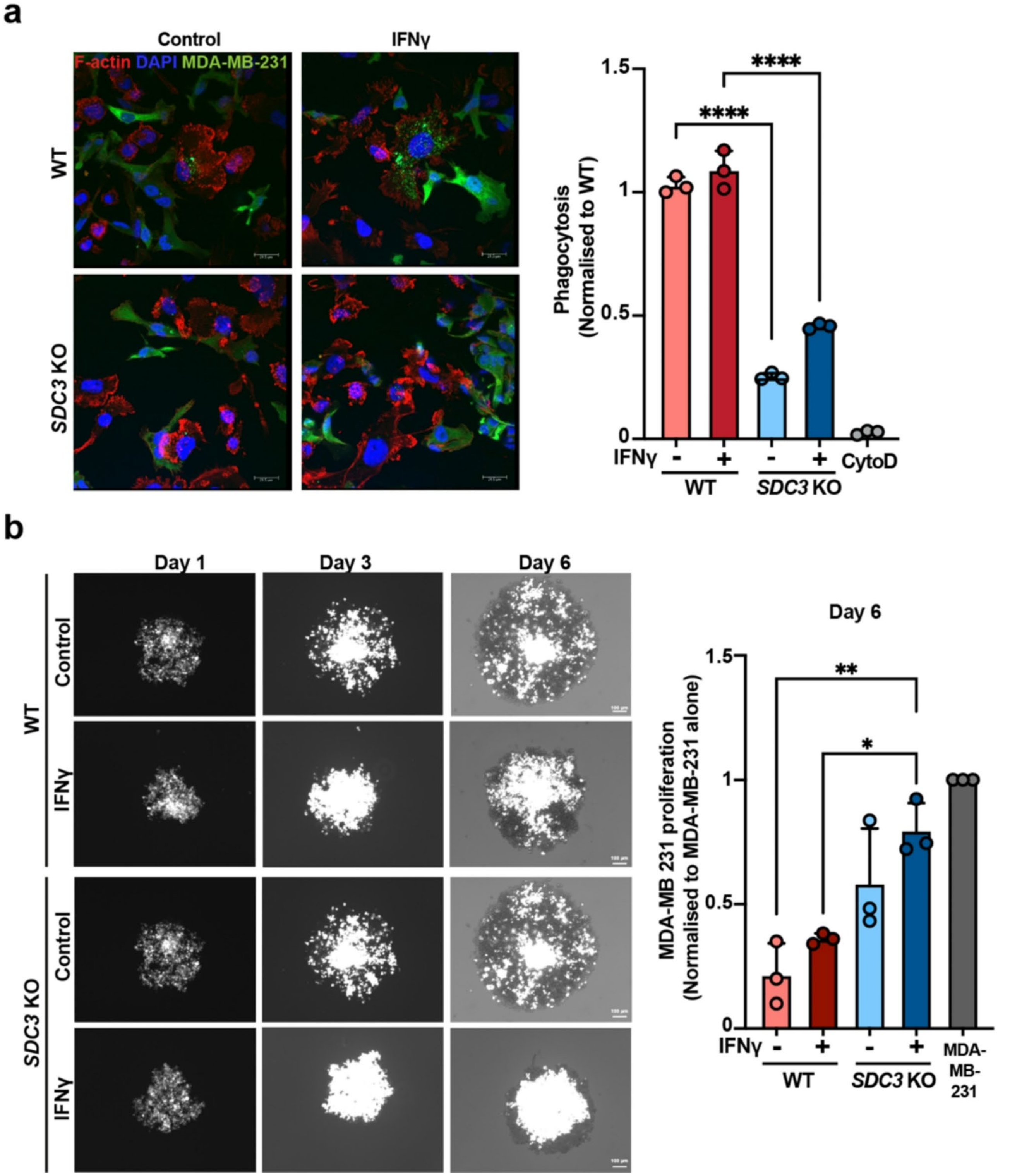

Fig. 4 SDC3 promotes macrophage phagocytic capacity and inhibits tumour-spheroid formation. (**a**) Left: Representative images of IFNγ-stimulated WT or *SDC3* KO THP-1 macrophages co-cultured with MDA-MB-231-GFP breast cancer cells. Images were taken with a Leica SP8 Lightning confocal microscope (scale bar 20.5 µm, *n*=3). Right: Quantification of phagocytosis rate by flow cytometry normalized to WT, using the inhibitor of actin polymerization Cytochalasin D as control (*n*=3). (**b**) Left: Representative images of IFNγ-treated WT or *SDC3* KO THP-1 macrophages forming spheroids with MDA-MB-231-GFP cells. Images were taken using Nikon Eclipse TD 100 microscope at the indicated times (scale bar 100 µm, white colour represents GFP$^+$ tumour cells). Right: Proliferation of MDA-MB-231-GFP $^+$ tumour cells in each condition normalized to MDA-MB-231 condition, calculated after acquiring single cell suspensions of spheroids by flow cytometry (*n*=3). Means ± SEM. Statistically significant difference from controls or between indicated groups is shown by $*p<0.05$, $**p<0.01$ and $****p<0.0001$

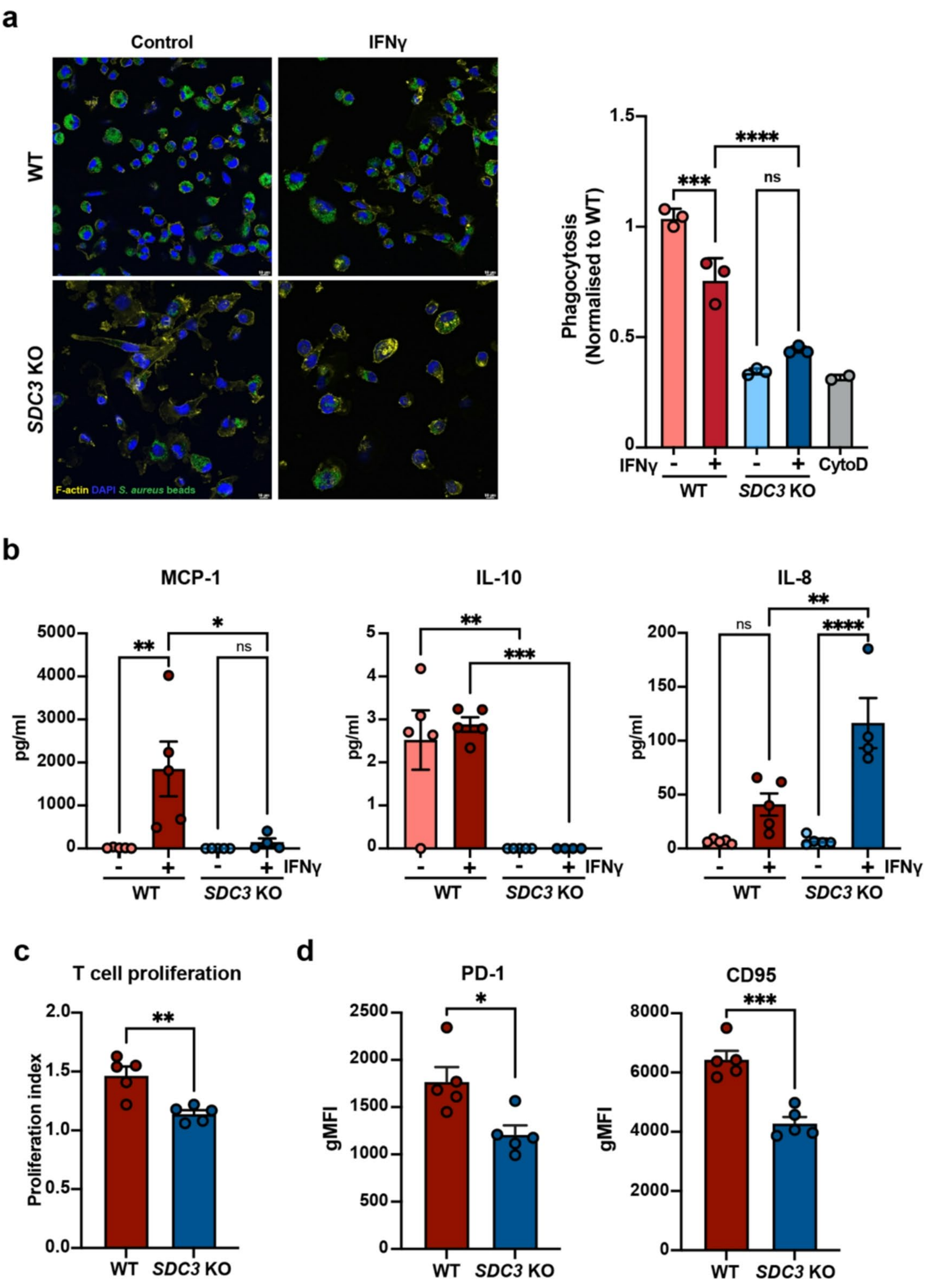

Fig. 5 SDC3 plays a role in macrophage pro-inflammatory functions. (**a**) Left: Representative confocal microscopy images of WT or *SDC3* KO THP-1 macrophages stimulated with 100 ng/ml of IFNγ and incubated with pHrodo™ Green *S. aureus* bioparticles. Images were taken using a Leica SP8 Lightning confocal microscope (scale bar 10 µm). Right: Flow cytometry quantification of *S. aureus* phagocytosis normalized to WT, using the inhibitor of actin polymerization Cytochalasin D as control ($n=3$). (**b**) Cytokine quantification in cell supernatants from WT or *SDC3* KO THP-1 macrophages stimulated with 100 ng/ml of IFNγ, using the LEGENDplex™ HU Essential Immune Response Panel ($n=5$). (**c**) Quantification of T cell proliferation index using CellTrace CFSE staining ($n=5$) in CD8$^+$ T cells co-cultured with IFNγ-treated WT or *SDC3* KO THP-1 macrophages. (**d**) Quantification of T cell activation markers PD-1 and CD95 by flow cytometry in CD8$^+$ T cells co-cultured with IFNγ-treated WT or *SDC3* KO THP-1 macrophages ($n=5$). Means ± SEM. Statistically significant difference from controls or between indicated groups is shown by ns: not significant, *$p<0.05$, **$p<0.01$, ***$p<0.001$ and ****$p<0.0001$

inhibited T cell proliferation (Fig. 5c) and reduced the activation of CD8$^+$ T cells, evidenced by a decrease in PD-1 and CD95 surface markers in T cells (Fig. 5d and Supplementary Fig. 5c). Together, these data support the notion that SDC3 is a central regulator of macrophage inflammatory functions and can modulate CD8$^+$ T cell activation. Given the essential role of pro-inflammatory cytokines and CD8$^+$ T cells as effectors of anticancer immune responses, SDC3 postulates as a possible target for cancer immunotherapies.

Syndecan-3 deficient macrophages promote angiogenesis *via* the release of pro-angiogenic factors

Vital for cancer progression and growth is tumour vascularization. Tumour angiogenesis involves the recruitment of new blood vessels that support tumour growth and promote metastasis and is orchestrated by a range of secreted factors and signalling pathways [44]. Since SDC3 has been previously ascribed a role during angiogenesis [45], and given the upregulation of angiogenesis pathways observed in *SDC3* KO macrophages (Fig. 3b), we investigated the potential influence of macrophage SDC3 in the regulation of blood vessel migration and growth. With this aim, we assessed the effect of IFNγ-stimulated WT or *SDC3* KO macrophage supernatants on the migration of Human Umbilical Vein Endothelial Cells (HUVECs), by measuring endothelial cell impedance in real-time (Fig. 6a). Media from IFNγ-stimulated *SDC3*-deficient macrophages promoted significantly higher migration of HUVECs, as compared to media from WT cells (Fig. 6b). Again, treatment with supernatants from unstimulated WT vs. KO macrophages showed no difference in HUVEC migration, suggesting that IFNγ-induced upregulation of SDC3 is critical for this effect. In an attempt to model the reorganization stage of the angiogenic process, we next measured the ability of endothelial cells to form capillary-like structures using the tube-formation assay (Fig. 6c). Here, conditioned medium from IFNγ-stimulated *SDC3*-deficient macrophages supported the formation of higher tube number compared to supernatants from WT macrophages (Fig. 6d).

VEGFA and its two tyrosine kinase receptors, VEGFR1 and VEGFR2, represent a key signalling pathway mediating physiological and pathological angiogenesis [34]. Its secretion by stromal cells and macrophages is a hallmark of tumour angiogenesis [46]. As such, we investigated VEGFA levels in the supernatants of IFNγ-stimulated WT or *SDC3* KO macrophages. Macrophages deficient for *SDC3* showed a significant increase in the secretion of VEGFA into the medium (Fig. 6e). Moreover, given the previously established role of VEGFA in the release of other pro-angiogenic markers [47], we analyzed the potential secretion of other angiogenic factors in IFNγ-stimulated WT or *SDC3* KO macrophages. Macrophages deficient for *SDC3* showed a significant increase in the secretion of PECAM-1 and IL-8 that, together with VEGFA, could account for the increased migration and tube formation observed in HUVECs (Fig. 6f). Collectively, *SDC3* deficient macrophages exerted a pro-migratory and proliferative effect on endothelial cells, suggesting a role for macrophage SDC3 during angiogenesis.

Discussion

Despite our growing understanding of the role of macrophages in the development and progression of tumours, details of the mechanisms that mediate this response remain unclear. Here, we have identified SDC3 as a modulator of macrophage functions, with potential implications in inflammation and tumour progression (Fig. 7). Specifically, we have demonstrated that SDC3 is expressed by macrophages in response to IFNγ, and that genetic ablation of this proteoglycan leads to altered macrophage functions, resulting in increased tumour cell proliferation. Mechanistically, SDC3 was necessary for the secretion of pro-inflammatory cytokines, activation of T cells, and inhibition of angiogenesis. These results present SDC3 as a positive regulator of pro-inflammatory/anti-tumour functions in macrophages.

The molecular regulation of macrophage functions is complex and multifactorial. While pro-inflammatory cytokines can trigger the activation of macrophages to unleash an effective inflammatory response, anti-inflammatory mediators can bias the fate of macrophages into a regulatory role in tissue homeostasis. The roles of SDC1, 2 and 4 as essential regulators of inflammation are well established [14], but details about the association of inflammation and SDC3 are scarce. Nonetheless, recent studies suggest that SDC3 is important for inflammatory disorders such as rheumatoid arthritis and infection [48–50]. Our findings demonstrated the expression of SDC3 in macrophages in response to the pro-inflammatory cytokine IFNγ, but not the anti-inflammatory cocktail IL-4/IL-13. *SDC3*-deficient macrophages neglected to show the archetypal shape of pro-inflammatory macrophages in response to IFNγ and exhibited, instead, a more rounded phenotype, a feature of undifferentiated macrophages [51]. In line with this, previous studies have explored the role of SDCs in cellular differentiation. For instance, glycosylated SDC1-4 ectodomains determine osteoclast differentiation through binding to M-CSF [52]. SDC4 has also been shown to be crucial for muscle cell differentiation, and SDC1 plays a role in endothelial cell differentiation [53, 54]. Notably, loss of *SDC3* did not impact the expression of the other members of the family, suggesting that the role of this proteoglycan in macrophage

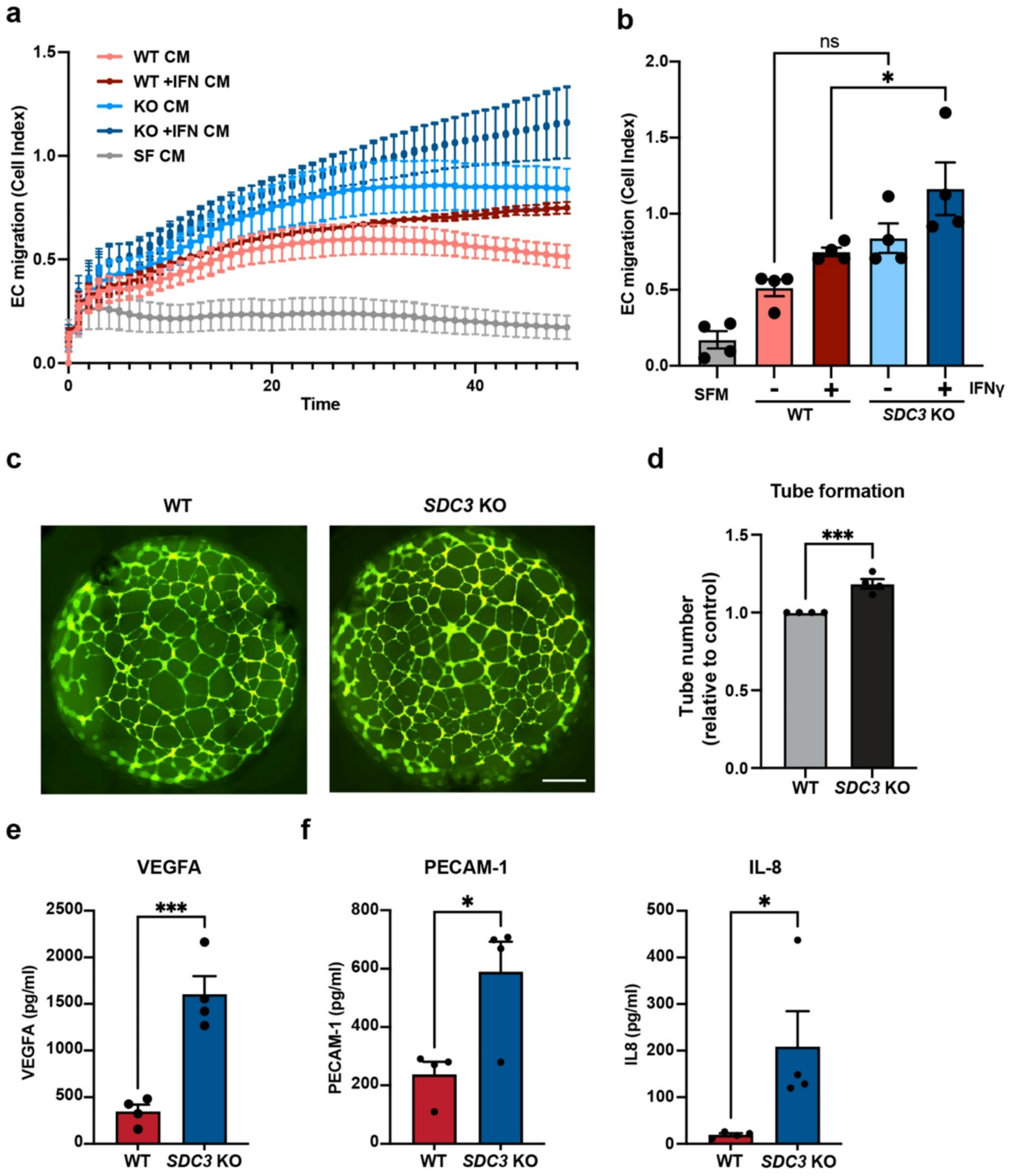

differentiation is mediated through SDC3-intrinsic mechanisms. The role of the SDC family in cellular differentiation could potentially be regulated through the interaction with ECM molecules [55]. Indeed, GAG substitutions on SDCs, through which binding to ECM molecules occur, are likely to be cell type and tissue dependent [45], accounting for the roles of SDCs in various cell types/tissues. SDC3 binding to the ECM could conceivably explain the mechanism by which it controls the phosphorylation of PYK2, RSK1/2/3 and HSP27. PYK2 is a key protein tyrosine kinase localized at podosomes, which are actin-rich structures present in highly motile cells such as macrophages. These structures

Fig. 6 SDC3 deficient macrophages regulate EC migration and tube formation. (**a**) HUVEC migration over the indicated times in response to conditioned media (CM) from WT or *SDC3* KO THP-1 macrophages stimulated with 100 ng/ml of IFNγ. Serum-free media (SFM) was used as negative control ($n=4$). (**b**) Quantification of HUVEC migration (Cell Index) shown in (a) at 48 h ($n=4$). (**c**) Representative images of Matrigel-grown HUVECs treated with supernatants from WT or *SDC3* KO THP-1 macrophages stimulated with 100 ng/ml of IFNγ. Tube formation was imaged using an Olympus IX-83 inverted microscope (scale bar 1 mm, $n=4$). (**d**) Quantification of total tube number shown in (c) at 24 h, relative to WT untreated control ($n=4$). (**e**) VEGFA quantification by ELISA in the supernatants of WT or *SDC3* KO THP-1 macrophages stimulated with 100 ng/ml of IFNγ ($n=4$). (**f**) Angiogenic factor quantification in cell supernatants from WT or *SDC3* KO THP-1 macrophages stimulated with 100 ng/ml of IFNγ, using the LEGENDplex™ HU Angiogenesis Panel 1 ($n=4$). Means ± SEM. Statistically significant difference from controls or between indicated groups is shown by ns: not significant, $*p<0.05$ and $***p<0.001$

are surrounded by actin filaments, and contain ECM-binding molecules and receptor tyrosine kinases (RTKs), among others [56]. SDC3 could potentially be localized at these structures, and therefore, upon loss of SDC3, binding to the ECM is lost and phosphorylation of PYK2 could increase, resulting in decreased adhesion and migration, in line with previously observed inhibition of phosphorylation of PYK2 in response to cell adhesion [57]. Furthermore, HSP27 has been found to form complex with actin, suggesting its potential presence within these structures [58], in line with co-localization of SDC3 and actin shown previously [59]. Finally, RTKs within podosomes could activate the RAS/ERK pathway, resulting in the phosphorylation of RSK1/2/3, supporting the expression of chemokines, cytokines, and other plasma membrane markers characteristic of M2 polarization [60], as observed here. Loss of SDC3 could concomitantly be activating RTKs through the release of growth factors, cytokines and chemokines, previously bound to the GAG chains of SDC3.

Changes in the shape of macrophages as a consequence of adhesive cues can lead to alterations of key molecular pathways that are responsible for regulating the pro-inflammatory or pro-healing state of these cells. Here, we discovered that the classical pro-inflammatory markers CD40 and CD86, characteristic of M1-like macrophages [37], were drastically reduced upon deletion of *SDC3*. Simultaneously, *iNOS* and *TNF* also showed a decreased gene expression, and MCP-1, a pro-inflammatory cytokine, was also reduced in the supernatants from *SDC3* KO macrophages. These data points towards a loss of M1-like/pro-inflammatory phenotype in *SDC3*-deficient macrophages. Phosphorylation of HSP27 was increased in *SDC3* KO macrophages, in line with previous roles for this kinase in the acquisition of M2-like phenotypes in TAMs [61]. Nevertheless, genes related to an M2-like/anti-inflammatory state such as CD206 or CD163 were not upregulated in *SDC3* KO macrophages. In line with this, an increase in the secretion of IL-8, a classical pro-inflammatory cytokine, was also observed upon loss of *SDC3*. Together, these results outline the simplicity of the historically assumed M1/M2-paradigm, and support the current prevailing macrophage spectrum model, in which M1 and M2 macrophages are present at the opposing ends of the spectrum, while other subtypes of macrophages are still present in between [62].

In analysing how SDC3 may influence the expression of other key genes related to macrophage functions, we observed an enrichment of pathways related to angiogenesis and protein secretion, while inflammatory responses and genes related with immune system recognition were downregulated. Accordingly, when investigating $CD8^+$ T cell functions upon co-culture with *SDC3* KO macrophages, a reduction in cell proliferation was observed, essential for $CD8^+$ T cell-mediated cancer cell cytotoxicity. In line with this, HSP27 phosphorylation, previously related to the induction of severe unresponsiveness in T cells [61], was also increased in *SDC3* KO macrophages. Our results further demonstrated a reduction of the immune checkpoint molecule PD-1 in $CD8^+$ T cells when co-cultured with *SDC3* KO macrophages, concomitant with an increased *PD-L1* gene expression in *SDC3*-deficient macrophages. CD86, besides a pro-inflammatory marker, is also a T cell co-stimulatory molecule [63], and was found downregulated in *SDC3* KO macrophages. Altogether, these data suggest that SDC3 in macrophages promotes the acquisition of an effector phenotype by T cells. Hypothesizing that SDC3 on macrophages may play a role in angiogenesis, we observed that *SDC3*-deficient macrophages promoted the migration and proliferation of endothelial cells. In line with this, thrombin-mediated cleavage of endothelial SDC3 has been reported to promote angiogenesis [29]. Nevertheless, a bacterially expressed GST fusion protein consisting of the entire mature SDC3 ectodomain has been shown to block angiogenesis in a number of in vitro and ex vivo models [64]. Given the lack of GAG substitutions in the bacterially generated SDC3 ectodomain, it is conceivable that the anti-angiogenic role of SDC3 is an intrinsic property of the core protein and, instead, the pro-angiogenic processes are dependent of GAG substitutions. In fact, heparan-sulphate, a type of GAG, is known to bind growth factors including VEGFA, PECAM-1 and IL-8 [65–67], which would suggest that in the absence of SDC3, an increase of free VEGFA, PECAM-1 and IL-8 would occur, in line with the observed increase in these angiogenic factors in the supernatants of *SDC3* KO macrophages shown here.

Notably, angiogenic, inflammatory and immune recognition processes are essential for TME-mediated tumour progression [46], proposing macrophage-derived SDC3 as a potential molecular basis for the regulation of tumour

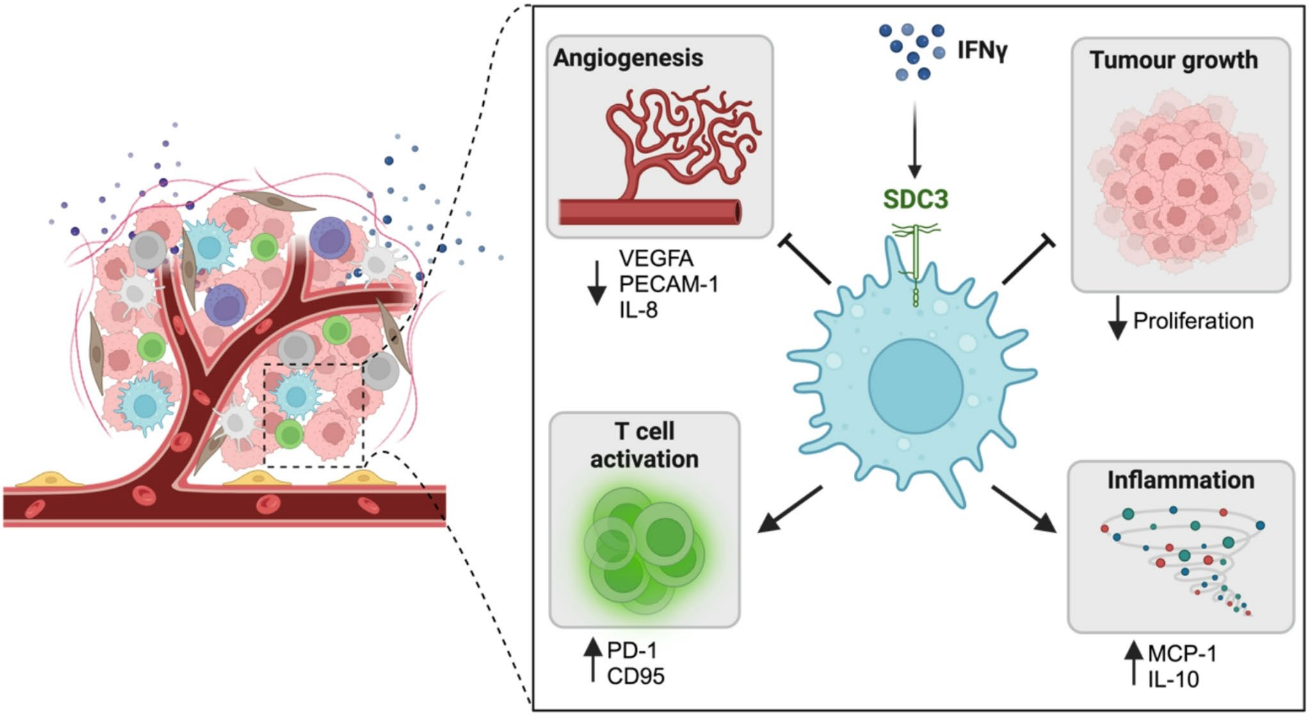

Fig. 7 Macrophage-derived SDC3 plays a role in the regulation of the TME. The plethora of cells present in the TME interact to promote or inhibit tumour progression and growth. SDC3 is expressed by macrophages in response to the pro-inflammatory cytokine IFNγ and regulates many aspects of the TME. Firstly, SDC3 in macrophages reduces tumour proliferation and is necessary for macrophage-mediated tumour-cell phagocytosis. The expression of SDC3 promotes a pro-inflammatory phenotype in macrophages that results in the secretion of cytokines such as MCP-1 and IL-10, while reducing the release of IL-8. Additionally, SDC3 is necessary for the acquisition of an effector phenotype by T cells, shown by an increased expression of PD-1 and CD95 on T cells. Finally, macrophage-derived SDC3 plays a role in the inhibition of endothelial cell migration and proliferation through a reduction in the secretion of angiogenic factors such as VEGFA, PECAM-1 and IL-8

progression. Indeed, macrophage-SDC3 was necessary for tumour cell phagocytosis and blocked tumour spheroid formation. Our results suggest that SDC3 could represent a promising strategy for targeting macrophages as novel immunotherapies. In this context, the development of agonistic antibodies against SDC3 could be a new therapeutic approach to increase the secretion of pro-inflammatory molecules, promote T cell activation and inhibit angiogenesis. Indeed, several clinical trials are currently undergoing targeting specific TAM molecules to enhance T cell activity and reduce tumour growth [8].

In summary, this work identifies SDC3 as a regulator of macrophage pro-inflammatory functions. Such a mechanism may promote bacterial phagocytosis and prevent tumour progression and growth. Mechanistically, we identified a SDC3-dependent regulation of pro-inflammatory cytokine and growth factor secretion. The involvement of SDC3 in T cell activation reveals a previously unidentified role for this proteoglycan in innate immune functions. Overall, our results suggest that targeting SDC3 could represent a promising strategy for solid tumours through the targeting of several key aspects of the TME.

Supplementary Information The online version contains supplementary material available at https://doi.org/10.1007/s00018-025-05649-1.

Acknowledgements This research was supported by the European Research Council (ERC) (ERC-2018-StG 804236-NEXTGEN-IO to AP), AECC (LABAE211744PALA to AP), La Caixa Foundation (LCF/PR/HR21/52410009 to AP) and the FERO Foundation. Personal fellowships: Lorena Pérez-Gutiérrez (Juan de la Cierva: JDC2022-048612-I, AECC Talent: TALEN245896PERE), Endika Prieto-Fernández (Ramón y Cajal: RYC2021-031213-I), Asier Antoñana-Vildosola (La Caixa Inphinit: LCF/BQ/DR20/11790022), Paloma Velasco-Beltrán (PRE2020-092342 funded by MCIN/AEI /10.13039/501100011033 and by FSE:"), Alexandre Bosch (AECC: PRDVZ19003BOSC), Borja Jimenez-Lasheras (Basque Government: PRE_2019_1_0320), Ander de Blas (AECC: PRDVZ21640DEBL), Jone Etxaniz-Díaz de Durana (PRE2022-104817 funded by MCIN/AEI /10.13039/501100011033 and by FSE+), Eunate Valdaliso-Díez (PREP2022-000848 funded by MICIU/AEI/10.13039/501100011033 and by ESF+), Alena Gros (Instituto de Salud Carlos III: MS15/00058) and Asís Palazón (RYC2018-024183-I funded by MCIN/AEI /10.13039/501100011033 and by FSE; and PID2022-139344OB-I00 funded by MCIN/ AEI /10.13039/501100011033/ and by FEDER.

Author contributions L.P-G, S.Y.L., and A.P. planned and executed experiments. L.P-G and A.P. conceptualized and wrote the manuscript. EP-M, L.E-M, A.A-V, P.V-B, A.B, A.B-M, B.J-L, A.B, J.E-DD, E.V-D, L.B-B, A.E., A.C., A.G. executed experiments and contributed

ideas. E.P-F, J.E.M and A.M.A performed RNAseq experiments and computational analysis. A.P. conceived and administered the project. All authors reviewed the manuscript.

Data availability RNA-Seq data sets generated in this publication are available in GEO database with the accession no. GSE273450: https://www.ncbi.nlm.nih.gov/geo/query/acc.cgi?acc=GSE273450. Enter token mfwrqgkmpxkpzub into the box.

Declarations

Ethical approval Buffy coats were provided by the Basque Biobank (www.biobancovasco.org) with appropriate approval of the Ethical and Scientific Committees (code CEIC E19-75).

Conflict of interest A.G. is a member of the scientific advisory board (SAB) of Achilles Therapeutics plc, SingulaBIO, RootPath, Inc., BioNTech SE, and consults is a consultant advisor for Instil BIo. AG is co-inventor of patents licensed and with royalties E-059-2013/0 E-085-2013/0, E-149-2015/0. The rest of the authors declare no potential conflicts of interest.

References

1. Hanahan D (2022) Hallmarks of cancer: new dimensions. Cancer Discov 12(1):31–46
2. Lin Y, Xu J, Lan H (2019) Tumor-associated macrophages in tumor metastasis: biological roles and clinical therapeutic applications. J Hematol Oncol 12(1):76
3. Goerdt S et al (1999) Alternative versus classical activation of macrophages. Pathobiology 67(5–6):222–226
4. Biswas SK, Mantovani A (2010) Macrophage plasticity and interaction with lymphocyte subsets: cancer as a paradigm. Nat Immunol 11(10):889–896
5. Pittet MJ, Michielin O, Migliorini D (2022) Clinical relevance of tumour-associated macrophages. Nat Rev Clin Oncol 19(6):402–421
6. Cheng S et al (2021) A pan-cancer single-cell transcriptional atlas of tumor infiltrating myeloid cells. Cell 184(3):792–809e23
7. Cassetta L et al (2019) Human Tumor-Associated macrophage and monocyte transcriptional landscapes reveal Cancer-Specific reprogramming, biomarkers, and therapeutic targets. Cancer Cell 35(4):588–602e10
8. Mantovani A et al (2022) Macrophages as tools and targets in cancer therapy. Nat Rev Drug Discov 21(11):799–820
9. Cassetta L, Pollard JW (2023) A timeline of tumour-associated macrophage biology. Nat Rev Cancer 23(4):238–257
10. Couchman JR (2003) Syndecans: proteoglycan regulators of cell-surface microdomains? Nat Rev Mol Cell Biol 4(12):926–937
11. Morgan MR, Humphries MJ, Bass MD (2007) Synergistic control of cell adhesion by integrins and syndecans. Nat Rev Mol Cell Biol 8(12):957–969
12. De Rossi G, Whiteford JR (2014) Syndecans in angiogenesis and endothelial cell biology. Biochem Soc Trans 42(6):1643–1646
13. Barbouri D et al (2014) Syndecans as modulators and potential Pharmacological targets in cancer progression. Front Oncol 4:4
14. Gopal S (2020) Syndecans in inflammation at a glance. Front Immunol 11:227
15. Alexopoulou AN, Multhaupt HA, Couchman JR (2007) Syndecans in wound healing, inflammation and vascular biology. Int J Biochem Cell Biol 39(3):505–528
16. Theocharis AD et al (2010) Proteoglycans in health and disease: novel roles for proteoglycans in malignancy and their Pharmacological targeting. Febs J 277(19):3904–3923
17. Iozzo RV, Sanderson RD (2011) Proteoglycans in cancer biology, tumour microenvironment and angiogenesis. J Cell Mol Med 15(5):1013–1031
18. Prieto-Fernández E et al (2020) Hypoxia promotes Syndecan-3 expression in the tumor microenvironment. Front Immunol 11:586977
19. García-Del Río A et al (2023) Factor-inhibiting HIF (FIH) promotes lung cancer progression. JCI Insight 8(20)
20. Korotkevich G et al (2021) Fast gene set enrichment analysis. bioRxiv, p. 060012
21. Liberzon A et al (2015) The molecular signatures database (MSigDB) hallmark gene set collection. Cell Syst 1(6):417–425
22. Dranoff G (2004) Cytokines in cancer pathogenesis and cancer therapy. Nat Rev Cancer 4(1):11–22
23. Gocher AM, Workman CJ, Vignali DAA (2022) Interferon-γ: teammate or opponent in the tumour microenvironment? Nat Rev Immunol 22(3):158–172
24. Suzuki A et al (2015) Targeting of IL-4 and IL-13 receptors for cancer therapy. Cytokine 75(1):79–88
25. Fitzgerald ML et al (2000) Shedding of syndecan-1 and–4 ectodomains is regulated by multiple signaling pathways and mediated by a TIMP-3-sensitive metalloproteinase. J Cell Biol 148(4):811–824
26. McWhorter FY et al (2013) Modulation of macrophage phenotype by cell shape. Proc Natl Acad Sci U S A 110(43):17253–17258
27. Pisconti A et al (2010) Syndecan-3 and Notch cooperate in regulating adult myogenesis. J Cell Biol 190(3):427–441
28. Shimazu A et al (1996) Syndecan-3 and the control of chondrocyte proliferation during endochondral ossification. Exp Cell Res 229(1):126–136
29. Jannaway M et al (2019) Thrombin-cleaved syndecan-3/-4 ectodomain fragments mediate endothelial barrier dysfunction. PLoS ONE 14(5):e0214737
30. Subramanian A et al (2005) Gene set enrichment analysis: a knowledge-based approach for interpreting genome-wide expression profiles. Proc Natl Acad Sci U S A 102(43):15545–15550
31. Arango Duque G, Descoteaux A (2014) Macrophage cytokines: involvement in immunity and infectious diseases. Front Immunol 5:491
32. Doroshow DB et al (2021) PD-L1 as a biomarker of response to immune-checkpoint inhibitors. Nat Rev Clin Oncol 18(6):345–362
33. Jeannin P et al (1999) Human effector memory T cells express CD86: a functional role in Naive T cell priming. J Immunol 162(4):2044–2048
34. Pérez-Gutiérrez L, Ferrara N (2023) Biology and therapeutic targeting of vascular endothelial growth factor A. Nat Rev Mol Cell Biol 24(11):816–834

35. Dooling LJ et al (2023) Cooperative phagocytosis of solid tumours by macrophages triggers durable anti-tumour responses. Nat Biomed Eng 7(9):1081–1096
36. Kim J, Koo BK, Knoblich JA (2020) Human organoids: model systems for human biology and medicine. Nat Rev Mol Cell Biol 21(10):571–584
37. Chen S et al (2023) Macrophages in immunoregulation and therapeutics. Signal Transduct Target Ther 8(1):207
38. Freeman SA, Grinstein S (2014) Phagocytosis: receptors, signal integration, and the cytoskeleton. Immunol Rev 262(1):193–215
39. Schütze S et al (2021) Interferon-gamma impairs phagocytosis of Escherichia coli by primary murine peritoneal macrophages stimulated with LPS and differentially modulates Proinflammatory cytokine release. Cytokine X 3(3):100057
40. Backman KA, Guyre PM (1994) Gamma-interferon inhibits Fc receptor II-mediated phagocytosis of tumor cells by human macrophages. Cancer Res 54(9):2456–2461
41. Wang Z et al (2015) Interferon-γ inhibits nonopsonized phagocytosis of macrophages via an mTORC1-c/EBPβ pathway. J Innate Immun 7(2):165–176
42. Deshmane SL et al (2009) Monocyte chemoattractant protein-1 (MCP-1): an overview. J Interferon Cytokine Res 29(6):313–326
43. Sanin DE, Prendergast CT, Mountford AP (2015) IL-10 production in macrophages is regulated by a TLR-Driven CREB-Mediated mechanism that is linked to genes involved in cell metabolism. J Immunol 195(3):1218–1232
44. Lugano R, Ramachandran M, Dimberg A (2020) Tumor angiogenesis: causes, consequences, challenges and opportunities. Cell Mol Life Sci 77(9):1745–1770
45. Arokiasamy S et al (2019) Syndecan-3 in inflammation and angiogenesis. Front Immunol 10:3031
46. Hanahan D, Weinberg RA (2011) Hallmarks of cancer: the next generation. Cell 144(5):646–674
47. Frezzetti D et al (2016) Vascular endothelial growth factor A regulates the secretion of different angiogenic factors in lung cancer cells. J Cell Physiol 231(7):1514–1521
48. Kehoe O et al (2014) Syndecan-3 is selectively pro-inflammatory in the joint and contributes to antigen-induced arthritis in mice. Arthritis Res Ther 16(4):R148
49. Eustace AD et al (2019) Soluble syndecan-3 binds chemokines, reduces leukocyte migration in vitro and ameliorates disease severity in models of rheumatoid arthritis. Arthritis Res Ther 21(1):172
50. de Witte L et al (2007) Syndecan-3 is a dendritic cell-specific attachment receptor for HIV-1. Proc Natl Acad Sci U S A 104(49):19464–19469
51. Italiani P, Boraschi D (2014) From monocytes to M1/M2 macrophages: phenotypical vs. Functional differentiation. Front Immunol 5:514
52. Kim JM et al (2018) Suppressive effect of syndecan ectodomains and N-desulfated heparins on osteoclastogenesis via direct binding to macrophage-colony stimulating factor. Cell Death Dis 9(11):1119
53. Rønning SB et al (2015) Syndecan-4 regulates muscle differentiation and is internalized from the plasma membrane during myogenesis. PLoS ONE 10(6):e0129288
54. Chung H et al (2016) Minireview: syndecans and their crucial roles during tissue regeneration. FEBS Lett 590(15):2408–2417
55. Streuli C (1999) Extracellular matrix remodelling and cellular differentiation. Curr Opin Cell Biol 11(5):634–640
56. Linder S et al (2023) Mechanisms and roles of podosomes and invadopodia. Nat Rev Mol Cell Biol 24(2):86–106
57. Duong LT, Rodan GA (2000) PYK2 is an adhesion kinase in macrophages, localized in podosomes and activated by beta(2)-integrin ligation. Cell Motil Cytoskeleton 47(3):174–188
58. Huot J et al (1996) HSP27 phosphorylation-mediated resistance against actin fragmentation and cell death induced by oxidative stress. Cancer Res 56(2):273–279
59. Berndt C et al (2001) Cloning and characterization of human syndecan-3. J Cell Biochem 82(2):246–259
60. Kerneur C, Cano CE, Olive D (2022) Major pathways involved in macrophage polarization in cancer. Front Immunol 13:1026954
61. Banerjee S et al (2011) Heat shock protein 27 differentiates tolerogenic macrophages that May support human breast cancer progression. Cancer Res 71(2):318–327
62. Nahrendorf M, Swirski FK (2016) Abandoning M1/M2 for a network model of macrophage function. Circ Res 119(3):414–417
63. Hathcock KS et al (1994) Comparative analysis of B7-1 and B7-2 costimulatory ligands: expression and function. J Exp Med 180(2):631–640
64. De Rossi G, Whiteford JR (2013) A novel role for syndecan-3 in angiogenesis. F1000Res 270
65. Ashikari-Hada S et al (2005) Heparin regulates vascular endothelial growth factor165-dependent mitogenic activity, tube formation, and its receptor phosphorylation of human endothelial cells. Comparison of the effects of heparin and modified heparins. J Biol Chem 280(36):31508–31515
66. Spillmann D, Witt D, Lindahl U (1998) Defining the interleukin-8-binding domain of Heparan sulfate. J Biol Chem 273(25):15487–15493
67. DeLisser HM et al (1993) Platelet/endothelial cell adhesion molecule-1 (CD31)-mediated cellular aggregation involves cell surface glycosaminoglycans. J Biol Chem 268(21):16037–16046